GLOBAL BIOGEOCHEMICAL CYCLES, VOL. 2, NO. 3, PAGES 279-288, SEPTEMBER 1988

CARBON AND HYDROGEN ISOTOPE FRACTIONATION RESULTING FROM ANAEROBIC METHANE OXIDATION

M. J. Alperin[1] and W. S. Reeburgh

Institute of Marine Science
University of Alaska, Fairbanks

M. J. Whiticar

Federal Institute for Geosciences and
Natural Resources, Hannover, Federal
Republic of Germany

Abstract. Methane oxidation in the anoxic sediments of Skan Bay, Alaska resulted in fractionation of carbon and hydrogen isotopes in methane. Isotope fractionation factors were estimated by fitting methane concentration, δ^{13}C-CH_4, and δD-CH_4 data with depth distributions predicted by an open system, steady state model. Assuming that molecular diffusion coefficients for $^{12}CH_4$, $^{13}CH_4$, and $^{12}CH_3D$ are identical, the predicted fractionation factors were 1.0088±0.0013 and 1.157±0.023 for carbon and hydrogen isotopes, respectively. If aqueous diffusion coefficients for the different isotopic species of methane differ significantly, the predicted fractionation factors are larger by an amount proportional to the diffusion isotope effect.

INTRODUCTION

Increasing concentrations of atmospheric methane have recently been reported [Rasmussen and Khalil, 1981; Blake et al., 1982; Rinsland et al., 1985; Blake and Rowland, 1988]. Ice core analyses demonstrate that the increase has been occurring for 200 to 300 years [Craig and Chou, 1982; Pearman et al., 1986]. Isotope mass balance models provide a powerful tool for elucidating the cause of the increase in atmospheric methane [Stevens and Engelkemeir, 1988]. These models exploit the fact that methane derived from different sources is often isotopically distinct.

Identification of atmospheric methane sources by isotope mass balance models requires knowledge of the kinetic isotope effect associated with atmospheric oxidation of methane by hydroxyl radical [Rust and Stevens, 1980; Davidson et al., 1987], as well as measurements of the isotopic composition of the methane emitted to the atmosphere from each potential source. A kinetic isotope effect arises because methane containing the lighter isotopes of carbon and hydrogen is oxidized slightly faster than methane containing the heavier isotopes [Bigeleisen and Wolfsberg, 1958]. The magnitude of this effect is expressed as an isotope fractionation factor (α), which may be defined as the ratio of relative reaction rates of molecules containing different isotopes [Rees, 1973]:

$$\alpha = \frac{R/c}{R^*/c^*} \quad (1)$$

where R is the reaction rate for a particular process, c is the concentration of reacting species, and the asterisk represents the molecule containing the heavier isotope.

In addition to knowledge of the kinetic isotope effect associated with the methane-hydroxyl reaction, information regarding isotope fractionation in methane prior to atmospheric release would be useful. This information would allow a quantitative assessment of the effect of consumption on the isotopic composition of methane.

The principal sink for methane prior to atmospheric release is bacterial oxidation, which can occur in both oxic and anoxic environments [Hanson, 1980; Reeburgh, 1980]. Methane oxidation by aerobic bacteria has been studied extensively in the laboratory, but the significance of its role in the global methane cycle is uncertain. Isotope fractionation factors, ranging from 1.005 to 1.031 for carbon and 1.103 to 1.325 for hydrogen, have been measured by culturing aerobic methylotrophs in a closed system, and monitoring changes in stable isotope ratios in either methane or the products of oxidation, CO_2 and H_2O [Silverman and Oyama, 1968; Barker and Fritz, 1981; Coleman et

[1]Now at Curriculum in Marine Sciences, University of North Carolina, Chapel Hill.

Paper number 8J0357.
0886-6236/88/008J-0357$10.00

al., 1981]. Since fractionation factors may be a function of physiological as well as environmental variables, kinetic isotope effects calculated from laboratory experiments may not be directly applicable to environmental data.

Methane oxidation by anaerobic bacteria is still considered controversial because organisms responsible for the process have not been isolated. Despite the lack of an isolated organism, a body of geochemical data suggests that anaerobic methane oxidation occurs [Alperin and Reeburgh, 1984] and may be a globally significant process [Henrichs and Reeburgh, 1987]. Anaerobic methane oxidation appears to be a nearly quantitative sink for methane in subtidal, anoxic marine sediments where ebullition is absent [Reeburgh, 1976; Alperin and Reeburgh, 1984]. The effects of anaerobic methane oxidation have been observed in numerous anoxic marine sediments [Reeburgh and Heggie, 1977; Martens and Berner, 1977; Reeburgh, 1980; Iversen and Blackburn, 1981; Devol, 1983; and others] and include a large shift in carbon stable isotope ratios of methane [Doose, 1980; Oremland and DesMarais, 1983; Alperin and Reeburgh, 1984; Whiticar and Faber, 1986].

The fractionation factors resulting from methane oxidation by anaerobic bacteria have not been measured in the laboratory because of the absence of enrichment cultures. This study estimates carbon and hydrogen isotope fractionation factors resulting from anaerobic methane oxidation by modeling measured distributions of isotope ratios in anoxic marine sediments. In contrast to the laboratory measurements for aerobic methane oxidation, fractionation factors estimated by this approach have the advantage of being directly applicable to the environment from which the isotope ratio distributions were derived.

METHODS

Study Site

Sediment was collected from Skan Bay (57°N, 167°W), a silled (10 m) embayment on the northwest side of Unalaska Island in the Aleutian Chain [Hattori et al., 1978]. During the summer, stable temperature and salinity gradients are established in the upper 30 m, leading to oxygen depletion within the water column. By September, bottom water oxygen concentrations are less than 10% of the air-saturated value.

The deep basin of Skan Bay (65 m) is a relatively isothermal environment. Bottom water temperatures in late September are about 3°C. Air temperature records indicate that the September bottom water temperature represents the annual maximum and also suggest that bottom water is unlikely to cool below 1°C during the winter. Thus, the annual temperature range within the sediment is on the order of 2°C.

The data included in this paper come from sediment collected in September 1984. Sediment was sampled by box coring followed by subcoring with 6.6-cm-ID Plexiglas core liner. The sediment appeared jet black from the interface down to 40 cm and dark grey thereafter. Hydrogen sulfide was abundant in samples near the sediment surface, indicating anoxia at or just below the sediment-water interface. After core retrieval, methane bubbles formed at depths greater than 30 cm. Ebullition was minimized by gentle but rapid handling of subcores.

Methane Concentrations and Stable Isotope Ratios

Subcores were sampled by extruding the sediment upward into a 3-cm segment of core liner. A metal shim was inserted beneath the segment and the sediment was quickly transferred to a N_2-flushed 600-mL lacquered steel can (#303). The 0–3 cm segment, which was composed of high-porosity flocculent material, was transferred to the can using a 50-mL plastic syringe with the tip partially removed. Methane bubble formation gave sediment below 30 cm a porous texture and may have led to some methane loss.

The cans were sealed using an Ives-Way Can Sealer, model #500 (Ives-Way Products, Inc., Buffalo Grove, Illinois). The entire process of sampling and canning was completed within 3 hours of the time the box core was taken. The cans were stored frozen (−10°C) until analysis (1 to 1.5 years). Six cans filled with 60 mL N_2-purged distilled water served as procedural blanks.

Methane was flushed from the can using a headspace sampler shown in Figure 1. This device consists of an upper plate fitted with an O ring, a recessed lower plate for positioning the can, and three threaded rods equipped with wing nuts to hold the plates together. The cans were penetrated by forcing sharpened cannulae through the lid. Quantitative recovery of known amounts of methane injected into the can demonstrated that the headspace sampler provided gas tight penetration.

The headspace sampler was attached to a combustion line. Methane was flushed from the can by circulating ultrapure N_2 through the sample (100 mL min^{-1}) with a Metal Bellows pump. Water was removed by a trap cooled to −89°C (2-propanol slurry), and CO_2 stripped from the pore water was collected in two serial liquid nitrogen traps. Blanks and methane standards run with and without CO_2 present were quantitatively and isotopically identical, indicating that negligible amounts of CO_2 were escaping the two traps.

Methane was combusted to CO_2 and H_2O by passage through a 25 cm × 16.6 cm ID Vycor tube packed with CuO wire heated to 800°C. Combustion efficiency of greater than 99.9% was shown by attaching a flame ionization detector to the effluent of the combustion tube. The combustion products were collected in two traps cooled with liquid nitrogen. Tests showed that the two traps in series collected 100.1±0.4% (n=4) of the CO_2.

Following a 40-min stripping period, noncondensible gases were pumped from the combustion line. The CO_2 was transferred to a reservoir of known volume and quantified manometrically while the H_2O was captured in a trap cooled to −89°C. The CO_2 and H_2O were flame-sealed in separate Pyrex tubes for carbon and hydrogen isotope ratio analyses. The H_2O was subsequently transferred to a Pyrex tube containing zinc catalyst and was quantitatively reduced to H_2 [Coleman et al., 1982].

Methane concentrations were calculated from the quantity of CO_2 recovered and the mass of wet sediment con-

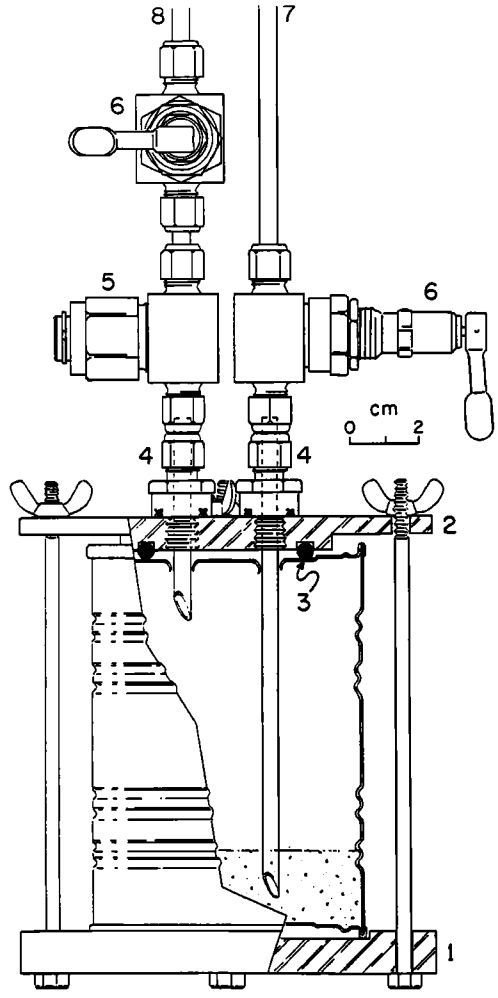

Fig. 1. Headspace sampler for removal of methane from the can. Numbered features are as follows: 1, lower plate; 2, upper plate; 3, 2″× 3/16″ silicone O ring; 4, bored-through 1/4″ O seal straight thread connector (Swagelok); 5, inline filter (Nupro) with 60-μm sintered stainless steel element; 6, toggle-operated bellows valve (Nupro); 7, inlet cannula (1/4" stainless steel tubing sharpened to a point on the end); 8, outlet cannula.

tained in the can. The following relationship was used to convert data to pore water concentration units:

$$[CH_4](mM) = \frac{\mu mol\ CO_2}{g\ \text{wet sediment}} \frac{\rho}{\phi}$$

The porosity (ϕ) and wet sediment density (ρ) were measured on replicate subcores.

Carbon and hydrogen stable isotope ratios were measured by ratio mass spectrometry. Results are reported using the standard "del" notation:

$$\delta(^o/_{oo}) = \left[\frac{R(\text{sample})}{R(\text{standard})} - 1\right]1000 \quad (2)$$

where R is the ratio of heavy to light isotope in the sample or the reference standard. The reference standard for carbon is Pee Dee Belemnite [Craig, 1957]; the standard for hydrogen is Standard Mean Ocean Water [Hagemann et al., 1970].

This analysis is not specific for methane, but includes any combustible compound having a significant vapor pressure at liquid nitrogen temperature (−196°C). Fortunately, nonmethane combustible gases that do not quantitatively condense in liquid nitrogen are rare; carbon monoxide and ethane are the two gases most likely to be present in recently deposited coastal sediments. There are no data on carbon monoxide concentrations in subtidal anoxic marine sediment, but it is likely that they are negligible relative to methane. Likewise, the ratio of ethane to methane is less than 10^{-3} in sediments similar to Skan Bay, where the methane is of biogenic origin [Bernard et al., 1977; Whiticar and Faber, 1986].

Standards and Blanks

Standards were analyzed by injecting 2 to 400 μmol of pure CH_4 (equivalent to concentrations ranging from 0.025 to 5 mM) into cans filled with 100 mL buffered solution (pH 7) containing 50 mM $NaHCO_3$. The bicarbonate served to mimic the dissolved inorganic carbon present in the pore water. The average recovery for standards larger than 6 μmol was 100±2% (n=11). The precision of the $\delta^{13}C$ and δD analyses for these standards was $\pm 0.1^o/_{oo}$ (n=11) and $\pm 5.5^o/_{oo}$ (n=5), respectively. Neither the recovery nor the $\delta^{13}C$ showed any systematic variation with the quantity of CH_4 added. However, δD values became isotopically heavier with decreasing sample size, presumably due to an H_2O blank. The magnitude of this blank effect was less than $10^o/_{oo}$, which is small relative to natural variation in δD-CH_4 within the sediment.

Blanks and samples or standards containing less than 6 μmol CH_4 (equivalent to concentrations below 0.075 mM) could not be quantified manometrically. Alternatively, pressures were measured with a thermocouple gauge calibrated against CO_2. Although accuracies of standards containing less than 6 μmol CH_4 were low, recoveries were 80 to 100%.

Carbon blanks for the methane analysis were 0.24± 0.04 μmol (n=6), which was insufficient gas for an isotope ratio analysis. The $\delta^{13}C$ of the methane blank was calculated to be $-34.4^o/_{oo}$ by extrapolation to 100% of a plot of $\delta^{13}C$-CH_4 versus percent blank for standards containing less than 6 μmol CH_4. Sample carbon isotope ratios were corrected for this blank contribution by a mass balance calculation. The magnitude of the correction was less than $0.5^o/_{oo}$ except for samples within 6 cm of the sediment-water interface, where the correction was $1–2^o/_{oo}$. The quantity of methane recovered from the 0–3 cm sediment interval was insufficient for isotope ratio analysis.

RESULTS

Depth distributions of methane concentrations and carbon and hydrogen stable isotope ratios are shown in Figure 2. Methane concentration profiles are concave up above 30 cm, a common characteristic of profiles from anoxic marine sediments [Reeburgh and Heggie, 1977]

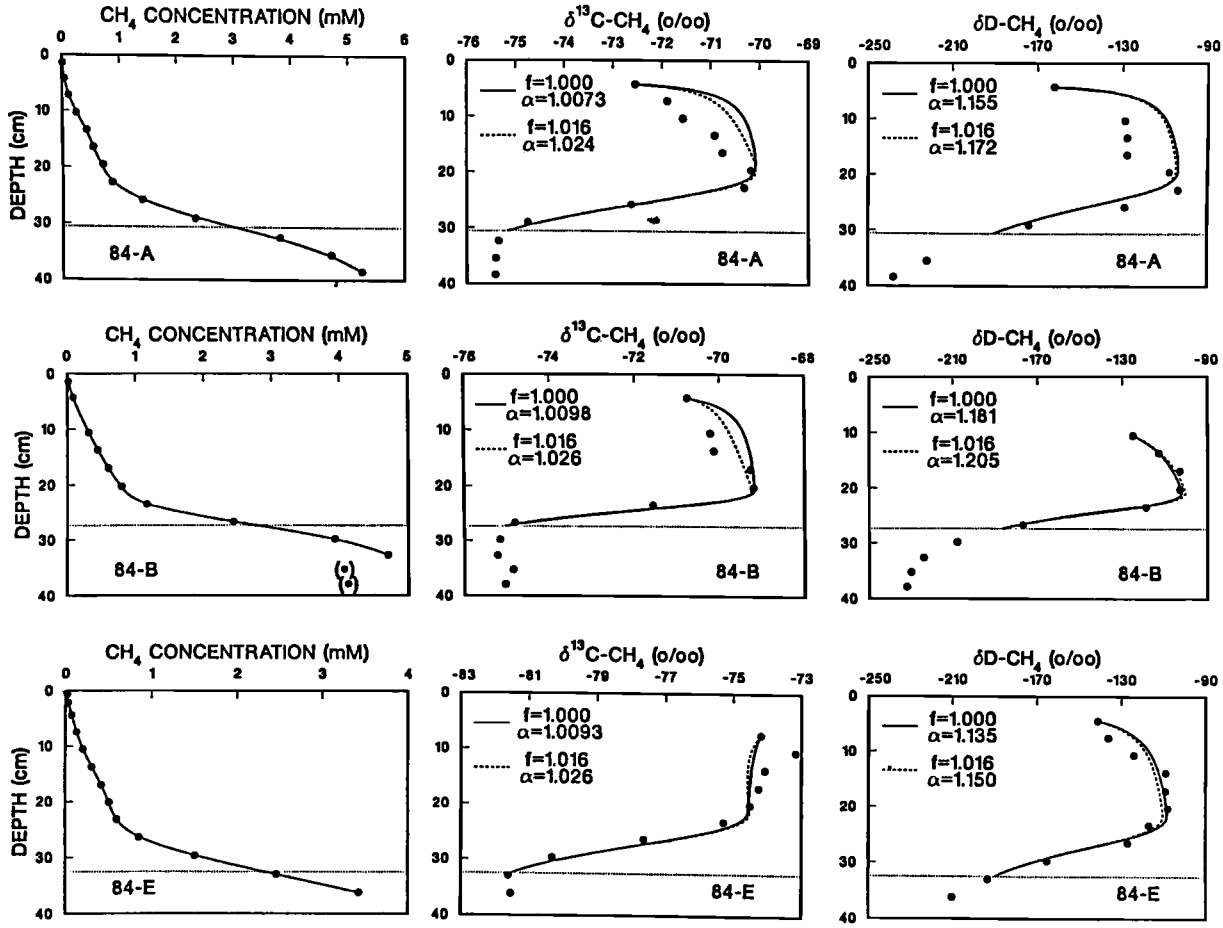

Fig. 2. Depth distributions of CH_4 concentration, $\delta^{13}C$-CH_4, and δD-CH_4. The solid circles represent the midpoint of the depth interval sampled. Subcores 84-A and 84-B are replicates from a single box core; subcore 84-E is from a second box core taken at approximately the same location. Solid and dashed curves represent cubic splines fit to the concentration data or model-derived $\delta^{13}C$-CH_4 and δD-CH_4 profiles, while horizontal dotted lines mark the base of the methane oxidation zone (see the section on isotopic fractionation models). Definitions of f and α are provided in the text. Concentration measurements bracketed by parentheses are assumed to be unreliable due to methane bubble formation after core retrieval. Note changes in methane concentration and $\delta^{13}C$-CH_4 scale for each subcore.

indicating net methane consumption [Reeburgh, 1976; Martens and Berner, 1977]. The concentration profiles change curvature and become linear or slightly concave down below 30 cm, suggesting net methane production in this zone.

Methane $\delta^{13}C$ values are relatively constant below 30 cm and become isotopically heavier between 30 and 20 cm as the methane concentration decreases. A similar shift in $\delta^{13}C$-CH_4 has been reported in other studies [Doose, 1980; Oremland and DesMarais, 1983; Alperin and Reeburgh, 1984; Whiticar and Faber, 1986] and has been attributed to the kinetic isotope effect associated with methane oxidation: $^{12}CH_4$ is oxidized at a faster rate than $^{13}CH_4$ leaving the residual methane isotopically heavier. The direction of the shift in $\delta^{13}C$-CH_4 reverses above 20 cm for two of the three subcores. Possible causes for this reversal are discussed below.

Methane δD and $\delta^{13}C$ profiles are similar in shape. There is a dramatic shift in δD-CH_4 values between 40 and 20 cm as they become isotopically heavier by more than $100^o/_{oo}$. There is also a reversal in the direction of the δD-CH_4 shift above 20 cm, as was seen in two of the three $\delta^{13}C$-CH_4 profiles. Throughout the sediment column, the δD-H_2O of the pore water was uniform at $-5\pm2^o/_{oo}$.

ISOTOPE FRACTIONATION MODELS

Rayleigh Models

Rayleigh distillation equations have been used extensively to model stable isotope fractionation in natural systems [Broecker and Oversby, 1970; Claypool and Kaplan, 1974]. These models assume that isotope fractionation is analogous to a distillation: molecules containing

the lighter isotopes react or "distill" preferentially leaving the unreacted reservoir isotopically heavier. The isotope fractionation factor for anaerobic methane oxidation has been estimated by applying Rayleigh models to $\delta^{13}C$-CH_4 data from a variety of sedimentary environments. Alperin and Reeburgh [1984] predicted a fractionation factor for anaerobic methane oxidation of 1.004, while estimates of Whiticar and Faber [1986], which may include the effects of aerobic as well as anaerobic oxidation, range from 1.002 to 1.014.

The Rayleigh model assumes that isotope fractionation associated with methane oxidation is the only process influencing the isotope ratio depth distributions. However, natural sediments are open systems, and isotope fractionation models of pore water methane profiles should take account of diffusive transport. Diffusion can influence isotope ratio depth distributions in two ways. First, the kinetic isotope effect leads to preferential oxidation of isotopically light methane, thereby steepening the concentration gradient and enhancing the diffusive flux of light methane relative to heavy methane [Jørgensen, 1979; Goldhaber and Kaplan, 1980; Chanton et al., 1987]. Second, diffusion coefficients for $^{12}CH_4$, $^{13}CH_4$, and CH_3D may differ. This latter point is discussed below.

Diagenetic Models

Berner [1980] derived a theoretical equation that describes the concentration-depth distribution of a pore water constituent as a function of diffusion, sediment accumulation, compaction, and reaction:

$$\phi^2 D_o \frac{d^2c}{dx^2} + \left(3\phi D_o \frac{d\phi}{dx} - \frac{\omega_\infty \phi_\infty}{\phi}\right)\frac{dc}{dx} + R_x = 0 \qquad (3)$$

where c is pore water concentration, x is depth below the sediment surface, D_o is the free solution diffusion coefficient (which is related to the whole sediment diffusion coefficient following Ullman and Aller [1982]), ϕ is porosity, ω is burial velocity of solid particles relative to the sediment-water interface, the subscript (∞) represents the depth where the porosity gradient approaches 0, and R_x is the depth dependent reaction rate. This form of the diagenetic equation is derived by Murray et al. [1978].

The significant assumptions involved in application of (3) are (1) the system is at steady state with respect to methane; (2) molecular diffusion and sedimentation are the dominant transport processes for methane; and (3) the increase in methane concentration with depth is large compared to horizontal concentration gradients. Under these conditions, (3) provides a numerical representation of the $^{12}CH_4$ concentration-depth distribution. Likewise, an analogous equation for isotopically heavy methane ($^{13}CH_4$ or CH_3D) can be written

$$\phi^2 \frac{D_o}{f}\frac{d^2c^*}{dx^2} + \left(3\phi \frac{D_o}{f}\frac{d\phi}{dx} - \frac{\omega_\infty \phi_\infty}{\phi}\right)\frac{dc^*}{dx} + R_x^* = 0 \qquad (4)$$

where c^* and R_x^* are the concentration and reaction rate for the isotopically heavy species, respectively, and f represents the molecular diffusivity ratio (light:heavy) for isotopic species. Substituting (1) into (4), and assuming that α is constant with depth,

$$\phi^2 \frac{D_o}{f}\frac{d^2c^*}{dx^2} + \left(3\phi \frac{D_o}{f}\frac{d\phi}{dx} - \frac{\omega_\infty \phi_\infty}{\phi}\right)\frac{dc^*}{dx} + \left(\frac{R_x}{\alpha c}\right)c^* = 0 \qquad (5)$$

Model parameters whose values have been measured or estimated from the literature (D_o, ϕ, and ω_∞) are summarized in Table 1. If the $^{12}CH_4$ reaction rate (R_x) and diffusivity ratio for molecules containing light and heavy isotopes (f) are known, and a value for the fractionation factor (α) assumed, (3) and (5) can be numerically solved to yield depth distributions of isotopically light and heavy methane.

$^{12}CH_4$ Reaction Rate

The diagenetic equation provides a means of estimating the methane reaction rate from the methane concentration profile. Inversion of (3) shows that the depth dependent reaction rate (R_x) is a function of the first and second derivatives of the methane concentration profile:

$$R_x = -\phi^2 D_o \frac{d^2c}{dx^2} - \left(3\phi D_o \frac{d\phi}{dx} - \frac{\omega_\infty \phi_\infty}{\phi}\right)\frac{dc}{dx} \qquad (6)$$

First and second derivatives were estimated by differentiating a cubic spline fit to the methane concentration data. A cubic spline is a function consisting of multiple cubic polynomials joined together with the condition of continuous first and second derivatives [Cheney and Kincaid, 1980]. Ahlberg et al. [1967] have demonstrated that cubic splines provide reliable estimates of derivatives for a wide variety of functional shapes. Details of the spline fitting routine are available in the work by Alperin [1988].

The accuracy of model-predicted reaction rates was tested by comparison with methane oxidation rates measured by the $^{14}CH_4$ tracer technique [Alperin and Reeburgh, 1985]. A cubic spline was fit to the methane concentration data and the first and second derivatives estimated

TABLE 1. Model Parameters

Parameter	Value
ϕ	$0.135 \exp(-0.0929\ x) + 0.864$[a]
$d\phi/dx$	$-0.0126 \exp(-0.0929\ x)$
ϕ_∞	0.864[a]
ω_∞	1.0 ± 0.2 cm yr^{-1} [b]
D_o	8.0×10^{-6} cm^2 s^{-1} [c]

[a]Least squares fit of porosity versus depth data [Alperin, 1988] to an exponential function (r=0.95, n=39).
[b]Based on ^{137}Cs and ^{210}Pb geochronologies.
[c]From Sahores and Witherspoon [1970] corrected to in situ salinity using the Stokes-Einstein equation [Lerman, 1979].

by differentiating the spline function. The reaction rates were calculated according to (6) (Figure 3). The modeled rate distribution accurately reproduced the main features in the data: low rates near the surface, a mid-depth maximum in methane oxidation rate, and reduced rates at greater depth. Agreement between measured (oxidation) and modeled (production plus oxidation) rates suggests minimal methane production over the depth interval represented by these cores.

Cubic splines fit to the methane concentration data from subcores subjected to stable isotope analysis are shown in Figure 2. Reaction rates predicted by differentiating the spline functions show a distinct maximum in methane oxidation between 20 and 30 cm (Figure 4), in agreement with rates measured by the $^{14}CH_4$ tracer technique (Figure 3). Differences in the magnitude of the predicted rate

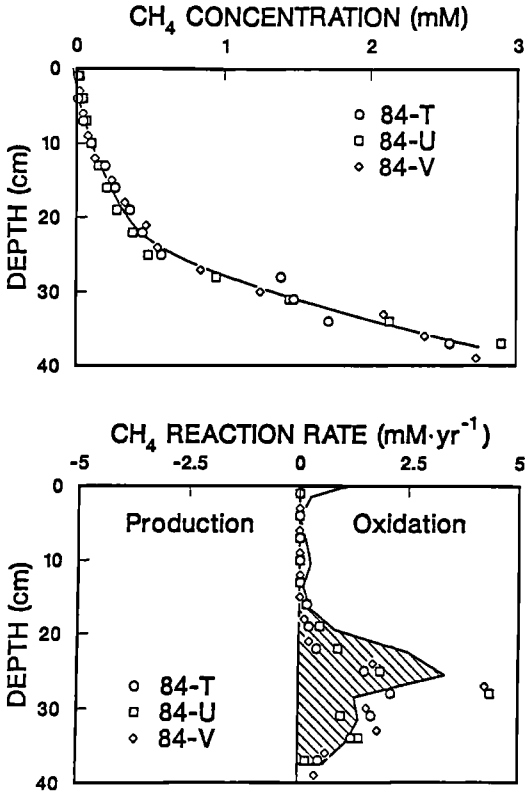

Fig. 3. Comparison of measured and modeled methane reaction rates. Upper panel: Symbols represent methane concentration data for three subcores from a single box core. Solid curve represents a cubic spline fit to the concentration data. Lower panel: Symbols represent methane oxidation rates determined by the $^{14}CH_4$ tracer technique. Solid curve represents the methane reaction rate predicted by differentiating the spline function fit to the concentration data. Positive rates indicate methane oxidation; negative rates indicate methane production. The zone of methane oxidation is represented by the hatched region. Methane concentration and oxidation rate data are from Alperin and Reeburgh [1985].

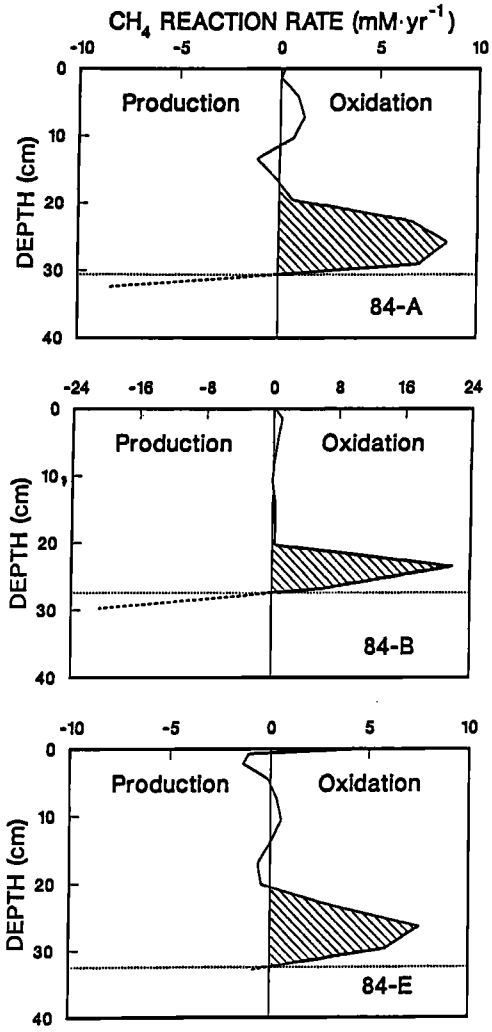

Fig. 4. Model-derived methane reaction rates for subcores subjected to stable isotope ratio analysis. Positive rates indicate net methane oxidation; negative rates indicate net methane production. The base of the methane oxidation zone (horizontal dotted line) is defined as the depth below which there is no further net oxidation. Methane reaction rate profiles incorporated into the diagenetic model (equations (3) and (5)) are represented by the hatched regions. Note changes in reaction rate scale for each subcore.

maxima between subcores are consistent with the variability in measured rates (compare subcores 84-T and 84-U, Figure 3) and appear to result from sediment heterogeneity.

High methane production rates begin just below the methane oxidation zone in subcores 84-A and 84-B (Figure 4). Subcore 84-E, like subcores 84-T, 84-U, and 84-V (Figure 3), apparently did not extend to the depth of the production zone.

The low-amplitude oscillations in the methane reaction rate above 20 cm (Figure 4, subcores 84-A and 84-E) reflect very subtle changes in curvature of the concentration

profile (Figure 2) and are not considered to be reliable estimates of in situ reaction rates. Therefore, reaction rates above the oxidation zone are taken as zero. These rates, which represent reaction of $^{12}CH_4$, $^{13}CH_4$, and $^{12}CH_3D$, are not significantly different from $^{12}CH_4$ reaction rates, since $^{12}CH_4$ represents about 99% of the total methane.

D_o for $^{13}CH_4$ and CH_3D

It is well established that gaseous diffusion coefficients for the different methane isotopic species vary inversely with the square root of their reduced masses [Mason and Marrero, 1970]. However, for methane in aqueous solution, the effect of isotopic substitution on the diffusion coefficient is uncertain. Diffusion coefficients for dissolved $^{13}CH_4$ and CH_3D have not been determined experimentally, and current theories of tracer diffusion in aqueous solution are inadequate for demonstrating either the presence or absence of a small isotope effect [Mills and Harris, 1976].

Of the available experimental data on aqueous diffusion coefficients for isotopically related solutes, CO_2 is probably the best methane analogue. O'Leary [1984] measured a small difference between $^{12}CO_2$ and $^{13}CO_2$ diffusion coefficients (f=1.0007±0.0002), suggesting that a measurable effect may exist for the different isotopic species of methane. However, the magnitude of this effect, which is probably strongly dependent on CH_4–H_20 molecular interactions, cannot be predicted. Therefore, we will consider two extreme cases: (1) aqueous diffusion coefficients for methane are unaffected by isotopic substitution (i.e., f=1.0000); and (2) CH_4–H_2O interactions are sufficiently small that diffusion coefficients for isotopic species follow the inverse square root reduced mass relationship applicable to a gaseous system (i.e., f=1.016).

Isotope Model Results

The diagenetic equations for isotopically light and heavy methane (equations (3) and (5)) were solved numerically using a finite difference method (IMSL Software Systems, Houston, Texas). These differential equations are second order and thus require two boundary conditions to define a unique solution. The upper boundary condition was established by the shallowest sample having sufficient methane for isotope ratio analyses. The lower boundary was set at the base of the methane oxidation zone, defined as the depth below which there is no further net oxidation (Figure 4). Solution of (3) and (5) yielded depth distributions of isotopically light and heavy methane, which were then used to calculate $\delta^{13}C$–CH_4 and δD–CH_4 profiles (equation (2)).

Sensitivity of the stable isotope model to α is shown in Figure 5. Note that these profiles are not the result of curve fitting an arbitrary function to the data. Rather, the curves represent solutions to the diagenetic equations (equations (3) and (5)). In the absence of an oxidation isotope effect (α=1.000), isotope ratio profiles are approximately constant from the base of the oxidation zone to within 10 cm of the sediment surface, where diffusive mixing at the upper boundary becomes important. A value of α greater than 1.000 produces a shift toward isotopically

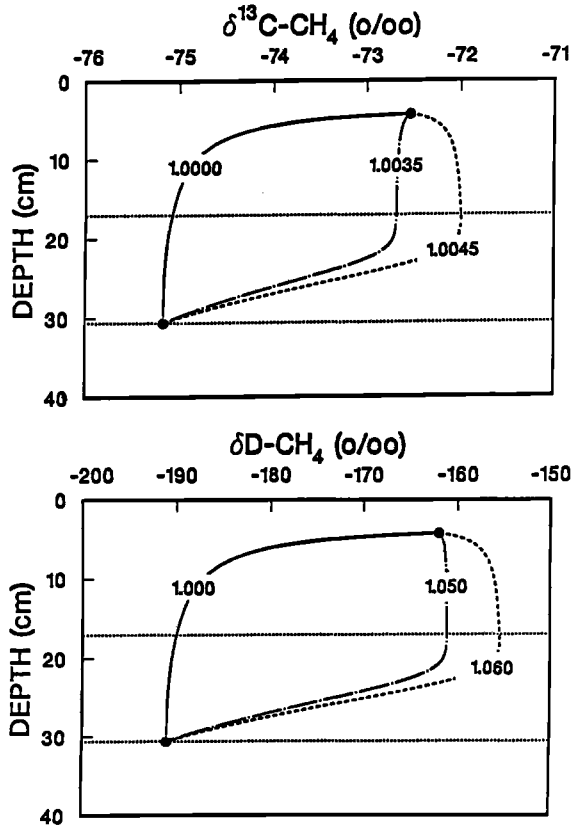

Fig. 5. Sensitivity of model-predicted $\delta^{13}C$-CH_4 and δD-CH_4 profiles to the magnitude of the isotope fractionation factor. The solid circles represent arbitrary boundary conditions. The curves represent predicted isotope ratio profiles for three values of α. The methane reaction rate profile is assumed to equal that of subcore 84-A (Figure 4). The region enclosed by the horizontal dotted lines marks the upper and lower boundaries of the methane oxidation zone. In this sensitivity analysis, diffusion coefficients for all isotopic species of methane are assumed to be equal (i.e., f=1.000).

heavier methane through the oxidation zone. The extent of this shift is quite sensitive to the magnitude of α; a change of ±0.001 shifts the predicted $\delta^{13}C$–CH_4 or δD–CH_4 profile by approximately ±0.5‰. Above the oxidation zone, $\delta^{13}C$–CH_4 and δD–CH_4 values are relatively constant until shallow depths where diffusive mixing occurs.

Results of applying the isotope model to the $\delta^{13}C$–CH_4 and δD–CH_4 data are shown in Figure 2. Isotope ratio profiles were predicted for two diffusion coefficient cases (f=1.000 and f=1.016). The steep $\delta^{13}C$–CH_4 and δD–CH_4 gradients through the methane oxidation zone represent the most robust portion of the data set. Therefore, values of α were adjusted until the model-predicted profiles reproduced the shift in $\delta^{13}C$–CH_4 and δD–CH_4 observed in the data. No attempt was made to fit the model-predicted profiles to isotope ratio data above the methane oxidation zone.

The magnitude of the predicted fractionation factors for carbon isotopes is strongly influenced by the ratio of diffusion coefficients for isotopically light and heavy species. In the absence of a diffusion isotope effect (f=1.000), predicted values range from 1.0073 to 1.0098; assuming that diffusion coefficients for different isotopic species of methane vary according to the inverse square root law (f=1.016) yields values ranging from 1.024 to 1.026.

The fractionation factor for hydrogen isotopes is an order of magnitude larger than for carbon. Hence, for CH_3D a diffusion isotope effect has a relatively small influence on the predicted fractionation factor. For the case of no diffusion isotope effect (f=1.000), predicted fractionation factors range from 1.135 to 1.181; assuming the maximum diffusion isotope effect (f=1.016) leads to α values ranging from 1.150 to 1.205.

Isotopically Light Methane at the Upper Boundary

The modeled $\delta^{13}C$–CH_4 and δD–CH_4 profiles generally reverse direction above the methane oxidation zone (Figure 2). This is caused by diffusive mixing of isotopically heavy methane from the oxidation zone and isotopically light methane present at the upper boundary. In subcore 84-E, the modeled $\delta^{13}C$–CH_4 profile does not reverse above the oxidation zone because methane at the top of the oxidation zone and the upper boundary have similar $\delta^{13}C$–CH_4 values.

Although the model reproduces the reversal in isotope ratio profiles seen in the data, it does not explain the cause of isotopically light methane at the upper boundary. Bottom water cannot be a significant source of isotopically light methane because concentrations are too low (0.0003 mM). Likewise, a diffusion isotope effect (larger diffusion coefficient for isotopically light species) can account for only a portion of the observed reversal.

The reversal in $\delta^{13}C$–CH_4 and δD–CH_4 values above 20 cm can be explained by production of isotopically light methane in the upper sediment. Approximately linear methane concentration profiles (Figure 2) and negligible methane oxidation rates (Figure 3) in the upper 20 cm indicate that methane production rates are slow relative to diffusion. The trend toward isotopically light methane in the shallow sediments may be due to a relatively slow input of methane highly enriched in the light isotopes. High sulfate reduction rates in this sediment region [Alperin and Reeburgh, 1985] suggest that this methane may be derived from a substrate not utilized by sulfate-reducing bacteria. Slow rates of methanogensis from methanol, a noncompetitive substrate with an extremely large carbon isotope effect ($\alpha > 1.070$) [Rosenfeld and Silverman, 1959; Krzycki et al., 1987], is a possible cause of the reversal observed in the isotope ratio data. If production of isotopically light methane is occurring within the methane oxidation zone, isotope fractionation factors predicted by the model will underestimate the in situ values.

CONCLUSIONS

1. Depth distributions of $\delta^{13}C$–CH_4 and δD–CH_4 from Skan Bay sediment demonstrate that anaerobic oxidation can significantly alter the carbon and hydrogen isotope ratios in methane.

2. An open system model that considers the effects of differential isotope diffusion and isotope fractionation resulting from oxidation successfully reproduces the major features in observed $\delta^{13}C$–CH_4 and δD–CH_4 profiles.

3. The accuracy of isotope fractionation factors predicted by the model is limited by the absence of data on diffusion coefficients for $^{13}CH_4$ and $^{12}CH_3D$. Consideration of two extreme cases, (1) no diffusion isotope effect and (2) a diffusion isotope effect approaching the theoretical maximum, demonstrate that predicted isotope fractionation factors depend on the magnitude of the diffusion isotope effect according to the following equation:

$$\alpha = \alpha_o + (f - 1)$$

where α is the in situ fractionation factor, α_o is the fractionation factor assuming no diffusion isotope effect, and f is the true value for the ratio of diffusion coefficients for isotopically light and heavy methane. Values of α_o, estimated by averaging model predicted fractionation factors for the f=1.000 case (Figure 2), are 1.0088±0.0013 (n=3) for carbon and 1.157±0.023 (n=3) for hydrogen.

4. Anaerobic methane oxidation appears to be a nearly quantitative sink for methane in environments where ebullition is absent. Hence, isotope fractionation resulting from anaerobic methane oxidation will not significantly affect isotope ratios in atmospheric methane. Anaerobic oxidation may influence the isotopic signature of methane entering the atmosphere from shallow marine environments where ebullition is the major mechanism of methane transport to the atmosphere.

Acknowledgments. We thank Jeff Chanton and Neal Blair for valuable discussions regarding diffusion isotope effects, and Dave DesMarais for a constructive review of an earlier version of this paper. Susan Sugai provided the geochronology data. Chirk Chu assisted in the computer programming. Samples for the work reported here were collected on cruise 062 of the R/V *Alpha Helix*. The work was supported by National Science Foundation grant OCN 8400864. Contribution number 674 from Institute of Marine Science, University of Alaska.

REFERENCES

Ahlberg, J., E. Nilson, and J. Walsh, *The Theory of Splines and Their Applications*, Academic, San Diego, Calif., 1967.

Alperin, M. J., The carbon cycle in an anoxic marine sediment: Concentrations, rates, isotope ratios, and diagenetic models, Ph.D. thesis, Univ. of Alaska, Fairbanks, 1988.

Alperin, M. J., and W. S. Reeburgh, Geochemical observations supporting anaerobic methane oxidation, in *Microbial Growth on C-1 Compounds*, edited by R. L. Crawford and R. S. Hanson, pp. 282–289, American Society for Microbiology, Washington, D. C., 1984.

Alperin, M. J., and W. S. Reeburgh, Inhibition experi-

ments on anaerobic methane oxidation, *Appl. Environ. Microbiol., 50,* 940–945, 1985.

Barker, J. F., and P. Fritz, Carbon isotope fractionation during microbial methane oxidation, *Nature, 293,* 289–291, 1981.

Bernard, B. B., J. M. Brooks, and W. M. Sackett, A geochemical model for characterization of hydrocarbon gas sources in marine sediments, *Proc. Annu. Offshore Technol. Conf., 9,* 435–438, 1977.

Berner, R. A., *Early Diagenesis: A Theoretical Approach,* 241 pp., Princeton University Press, Princeton, N. J., 1980.

Bigeleisen, J., and M. Wolfsberg, Theoretical and experimental aspects of isotope effects in chemical kinetics, *Adv. Chem. Phys., 1,* 15–76, 1958.

Blake, D. R., and F. S. Rowland, Continuing worldwide increase in tropospheric methane, 1978 to 1987, *Science, 239,* 1129–1131, 1988.

Blake, D. R., E. W. Mayer, S. C. Tyler, Y. Makide, D. C. Montague, and F. S. Rowland, Global increase in atmospheric methane concentrations between 1980 and 1982, *Geophys. Res. Lett., 9,* 477–480, 1982.

Broecker, W. S., and V. M. Oversby, *Chemical Equilibrium in the Earth,* 318 pp., McGraw-Hill, New York, 1970.

Chanton, J. P., C. S. Martens, and M. B. Goldhaber, Biogeochemical cycling in an organic-rich coastal marine basin, 8, A sulfur isotopic budget balanced by differential diffusion across the sediment-water interface, *Geochim. Cosmochim. Acta, 51,* 1201–1208, 1987.

Cheney, W., and D. Kincaid, *Numerical Mathematics and Computing,* 362 pp., Brooks/Cole, Monterey, Calif., 1980.

Claypool, G. E., and I. R. Kaplan, The origin and distribution of methane in marine sediments, in *Natural Gases in Marine Sediments,* edited by I. R. Kaplan, pp. 99–139, Plenum, New York, 1974.

Coleman, D. D., J. B. Risatti, and M. Schoell, Fractionation of carbon and hydrogen isotopes by methane-oxidizing bacteria, *Geochim. Cosmochim. Acta, 45,* 1033–1037, 1981.

Coleman, M. L., T. J. Shepard, J. J. Durham, J. E. Rouse, and G. R. Moore, Reduction of water with zinc for hydrogen isotope analysis, *Anal. Chem., 54,* 993–995, 1982.

Craig, H., Isotopic standards for carbon and oxygen and correction factors for mass-spectrometric analysis of carbon dioxide, *Geochim. Cosmochim. Acta, 12,* 133–149, 1957.

Craig, H., and C. C. Chou, Methane: The record in polar ice cores, *Geophys. Res. Lett., 9,* 1221–1224, 1982.

Davidson, J. A., C. A. Cantrell, S. C. Tyler, R. E. Shetter, R. J. Cicerone, and J. G. Calvert, Carbon kinetic isotope effect in the reaction of CH_4 with HO, *J. Geophys. Res., 92*(D2), 2195–2199, 1987.

Devol, A. H., Methane oxidation rates in the anaerobic sediments of Saanich Inlet, *Limnol. Oceanogr., 28,* 738–742, 1983.

Doose, P. R., The bacterial production of methane in marine sediments, Ph.D. thesis, Univ. of Calif., Los Angeles, 1980.

Goldhaber, M. B., and I. R. Kaplan, Mechanisms of sulfur incorporation and isotope fractionation during early diagenesis in sediments of the Gulf of California, *Mar. Chem., 9,* 95–143, 1980.

Hagemann, R., G. Nief, and E. Roth, Absolute isotopic scale for deuterium analysis of natural waters: Absolute D/H ratio for SMOW, *Tellus, 22,* 712–715, 1970.

Hanson, R. S., Ecology and diversity of methylotrophic organisms, *Adv. Appl. Microbiol., 26,* 3–39, 1980.

Hattori, A., J. J. Goering, and D. B. Boisseau, Ammonium oxidation and its significance in the summer cycling of nitrogen in oxygen depleted Skan Bay, Unalaska Island, Alaska, *Mar. Sci. Commun., 4,* 139–151, 1978.

Henrichs, S. M., and W. S. Reeburgh, Anaerobic mineralization of marine sediment organic matter: Rates and the role of anaerobic processes in the oceanic carbon economy, *Geomicrobiol. J., 5,* 191–237, 1987.

Iversen, N., and T. H. Blackburn, Seasonal rates of methane oxidation in anoxic marine sediments, *Appl. Environ. Microbiol., 41,* 1295–1300, 1981.

Jørgensen, B. B., A theoretical model of the stable sulfur isotope distribution in marine sediments, *Geochim. Cosmochim. Acta, 43,* 363–374, 1979.

Krzycki, J. A., W. R. Kenealy, M. J. DeNiro, and J. G. Zeikus, Stable carbon isotope fractionation by *Methanosarcina barkeri* during methanogenesis from acetate, methanol, or carbon dioxide-hydrogen, *Appl. Environ. Microbiol., 53,* 2597–2599, 1987.

Lerman, A., *Geochemical Processes: Water and Sediment Environments,* 481 pp., John Wiley, New York, 1979.

Martens, C. S., and R. A. Berner, Interstitial water chemistry of Long Island Sound sediments, I, Dissolved gases, *Limnol. Oceanogr., 22,* 10–25, 1977.

Mason, E. A., and T. R. Marrero, The diffusion of atoms and molecules, *Adv. At. Mol. Phys., 6,* 155–232, 1970.

Mills, R., and K. R. Harris, The effect of isotopic substitution on diffusion in liquids, *Chem. Soc. Rev., 5,* 215–231, 1976.

Murray, J. W., V. Grundmanis, and W. M. Smethie, Jr., Interstitial water chemistry in the sediments of Saanich Inlet, *Geochim. Cosmochim. Acta, 42,* 1011–1026, 1978.

O'Leary, M. H., Measurement of the isotope fractionation associated with diffusion of carbon dioxide in aqueous solution, *J. Phys. Chem., 88,* 823–825, 1984.

Oremland, R. S., and D. DesMarais, Distribution, abundance, and carbon isotopic composition of gaseous hydrocarbons in Big Soda Lake, Nevada: An alkaline, meromictic lake, *Geochim. Cosmochim. Acta, 47,* 2107–2114, 1983.

Pearman, G. I., D. Etheridge, F. de Silva, and P. J. Fraser, Evidence of changing concentrations of atmospheric CO_2, N_2O and CH_4 from air bubbles in Antarctic ice, *Nature, 320,* 248–250, 1986.

Rasmussen, R. A., and M. A. K. Khalil, Atmospheric methane (CH_4): Trends and seasonal cycles, *J. Geophys. Res., 86,* 9826–9832, 1981.

Reeburgh, W. S., Methane consumption in Cariaco Trench waters and sediments, *Earth Planet. Sci. Lett., 28,* 337–344, 1976.

Reeburgh, W. S., Anaerobic methane oxidation: Rate

depth distributions in Skan Bay sediments, *Earth Planet. Sci. Lett., 47,* 345–352, 1980.

Reeburgh, W. S., and D. T. Heggie, Microbial methane consumption reactions and their effect on methane distributions in fresh water and marine environments, *Limnol. Oceanogr., 22,* 1–9, 1977.

Rees, C. E., A steady-state model for sulphur isotope fractionation in bacterial reduction processes, *Geochim. Cosmochim. Acta, 37,* 1141–1162, 1973.

Rinsland, C. P., J. S. Levine, and T. Miles, Concentration of methane in the troposphere deduced from 1951 infrared solar spectra, *Nature, 318,* 245–249, 1985.

Rosenfeld, W. D., and S. R. Silverman, Carbon isotope fractionation in bacterial production of methane, *Science, 130,* 1658–1659, 1959.

Rust, F., and C. M. Stevens, Carbon kinetic isotope effect in the oxidation of methane by hydroxyl, *Int. J. Chem. Kinet., 12,* 371–377, 1980.

Sahores, J. J., and P. A. Witherspoon, Diffusion of light paraffin hydrocarbons in water from 2°C to 80°C, in *Advances in Organic Geochemistry, 1966,* pp. 219–230, edited by G. C. Spears, Pergamon, New York, 1970.

Silverman, M. P., and V. I. Oyama, Automatic apparatus for sampling and preparing gases for mass spectral analysis in studies of carbon isotope fractionation during methane metabolism, *Anal. Chem., 40,* 1833–1837, 1968.

Stevens, C. M., and A. Engelkemeir, Stable carbon isotopic composition of methane from some natural and anthropogenic sources, *J. Geophys. Res., 93*(D1), 725–733, 1988.

Ullman, W. J., and R. C. Aller, Diffusion coefficients in nearshore marine sediments, *Limnol. Oceanogr., 27,* 552–556, 1982.

Whiticar, M. J., and E. Faber, Methane oxidation in sediment and water column environments – Isotope evidence, *Org. Geochem., 10,* 759–768, 1986.

M. J. Alperin, Curriculum in Marine Sciences, 12-5 Venable Hall, University of North Carolina, Chapel Hill, NC 27599.

W. S. Reeburgh, Institute of Marine Science, University of Alaska, Fairbanks, AK 99775.

M. J. Whiticar, Federal Institute for Geosciences and Natural Resources, Stilleweg 2, 3000 Hannover 52, Federal Republic of Germany.

(Received December 14, 1987;
revised May 11, 1988;
accepted May 11, 1988.)